steel research international

Keyword

www.steel-research.de

Strain Aging Behavior of an Austenitic High-Mn Steel

Sebastian Wesselmecking, Wenwen Song, Yan Ma, Thorsten Roesler, Harald Hofmann, and Wolfgang Bleck*

The bake hardening treatment shows great potential for increasing the yield strength of steel components for automotive applications. This study investigates the effects of bake hardening on the yield strength and ductility of an austenitic high-Mn steel. In order to identify a promising process window, the prestrain, the bake hardening temperature, and the annealing time are varied. The bake hardening effect is evaluated by the uniaxial tensile tests with digital image correlation (DIC) in situ monitoring. The results show strong bake hardening effect on the high-Mn steel when certain amount of prestrain is applied. Large amounts of prestrain even leads to room temperature aging. Small angle neutron scattering (SANS) measurements indicate the absence of Mn–C short range ordering (SRO) after the prestrain; however, the nano-sized Mn–C SRO re-occurs after the annealing. At high prestrain degree, an increase in the number density of the Mn–C SRO is found in both cases, after annealing at elevated temperature and aging at room temperature, indicating an accelerated Mn–C SRO formation. The results suggest that SRO is responsible for an increase in the yield strength and a pronounced yielding of the high-Mn steel after bake hardening treatment.

1. Introduction

High-Mn steels possess an outstanding combination of ductility with high strength, which are of great interest for the automotive industry.[1] In particular, the extraordinary mechanical properties of high-Mn twining-induced-plasticity (TWIP) steels show the high-energy absorption potential to meet the requirements of crash relevant parts in automobiles.[2] A profound understanding of the deformation mechanisms in high-Mn TWIP steels in context of the stacking fault energy (SFE) and the influence of alloying elements was gained in many investigations.[3–6] To further increase the yield strength of high-Mn TWIP steels, different strategies have been pursued, such as micro-alloying with V and Nb.[7]

Bake hardening treatment – an aging treatment after prestrain – is widely applied in the automotive industry and able to increase both the yield strength and the elastic stiffness of components.[8–11] The high diffusion coefficient of body-centered cubic (b.c.c.) matrix highly promotes the bake hardening effect in ferritic steels. Bake hardening can be used as a beneficial heat treatment in austenitic steels to enhance the yield strength, but the underlying mechanism is unlikely to be the same as in the ferritic steels. Because the solubility of interstitials in face-centered cubic (f.c.c.) iron is higher and the diffusion coefficient is much lower.[12–15] Furthermore, the stress field around dislocations differs from an spherical symmetric distribution in f.c.c. phase to an asymmetric distribution in b.c.c. phase. The symmetric stress field in f.c.c. phase prevents interstitial atoms from locking dislocations.[16] A possible explanation for the phenomenon of strain aging in austenitic high-Mn steels is the interaction of dislocations and interstitial containing short-range orderings (SRO).[17] The SRO substructures locally decrease the internal energy and further increase the required stress for the movement of dislocations.[18] Previously, ab initio calculations were preformed to predict the local atomic ordering in the Fe–Mn–C system. The results indicate a SRO effect: carbon atoms prefer to occupy the octahedral sites of surrounding Mn atoms rather than Fe atoms.[19] The difference in energy for both antiferromagnetic and nonmagnetic structures between the Fe and the Mn octahedral was calculated to be 0.34 eV (33 kJ mol^{-1}).[19] This indicates a more stable structure in a short range ordered area, locally increasing the stability within the matrix and leading to an increase in strength. Recent investigations further indicated the SRO effect in the Fe–Mn–Al–C system.[20] The ab initio calculations suggested that Al is preferably located as a 2nd nearest neighbor of C. Moreover, it was found that the present of Al atoms has strong influence on the formation of Mn–C pairs. The SRO in high-Mn steels may act as an effective obstacle against dislocation glide, resulting in an increase in yield strength.[18] However, there is a little work of the bake hardening effect on the high-Mn steels.[21] Especially, the correlation between the bake hardening treatment and SRO formation is not well understood, which is of great importance to disentangling the underlying mechanisms of bake hardening effect in high-Mn steels.

In the present work, the effects of bake hardening treatment parameters on the mechanical properties of the steel Fe–19 wt% Mn–0.4 wt%C–2 wt%Cr–1wt%Al were systematically investigated. In addition, small angle neutron scattering (SANS) was employed to characterize the SRO in the materials. The effects of bake hardening treatment parameters on the SRO formation

S. Wesselmecking, Dr. W. Song, Y. Ma, Prof. W. Bleck
Steel Institute
RWTH Aachen University
Intzestraße 1, 52072 Aachen, Germany
E-mail: sebastian.wesselmecking@iehk.rwth-aachen.de

T. Roesler
thyssenkrupp Hohenlimburg GmbH
Oeger Straße 120, 58119 Hagen, Germany

Dr.-Ing. H. Hofmann
thyssenkrupp Steel Europe AG
Eberhardstraße 12, 44145 Dortmund, Germany

DOI: 10.1002/srin.201700515

were analyzed to sustain a thorough understanding of the bake hardening mechanisms in high-Mn steels.

2. Applied Methods

2.1. Material and Processing

The nominal chemical composition of the investigated steel is Fe–19 wt%Mn–0.4 wt%C–2 wt%Cr–1 wt%Al. The stacking fault energy (SFE) of the steel was calculated by means of a thermodynamics-based sub-regular solution model using the SGTE database.[22] The SFE was calculated to be 26 mJ m^{-2}; therefore, the TWIP effect is expected during plastic deformation at room temperature. The material was industrially processed. After continuous casting, the material was hot rolled, followed by cold rolling to a sheet thickness of 1 mm. Subsequently, the material was recrystallization annealed and skin-pass rolled with 2% reduction degree. Light optical microscopic observation of the materials after the skin-pass rolling was conducted with Klemm etching, as shown in **Figure 1**. The grain size was determined to be 3 μm.

2.2. Sample Preparation and Characterization Techniques

2.2.1. Tensile Tests and Baking Treatment

The uniaxial tensile tests were performed using a Zwick Z250 tensile test machine with a multiXtens strain measurement system. A constant strain rate 0.0025 s^{-1} was applied during the tensile tests. For the detailed analysis of the pronounced yielding phenomena, a 3D digital image correlation (DIC) system – GOM Aramis with a resolution of 12 Megapixel was used. In particular, the DIC system is very helpful to in situ characterize the local strain distribution and movement of the deformation bands during tensile tests. Flat specimen with an initial gauge length of 50 mm and a width of 12.5 mm referring to DIN 50125:2009–07 was retrieved.

The calculated BH-values represent the increase in strength caused by a bake hardening annealing after prestrain. The below used term "prestrain" describes the true plastic deformation ϕ applied on the tensile test sample within the first deformation process. To evaluate the BH-values, Equation 1 and 2 were used, in the cases of discontinuous and continuous transitions in the stress–strain curve, respectively.[23] In order to achieve reliable results, three parallel tests were conducted under each parameter set. As the reference state, three samples were prestrained and stored at room temperature for several hours until testing. In comparison, the bake hardening annealing was performed under various temperature and time conditions on another three samples. The latter state is named "with BH." Equation 1 and 2 denote the yield strength difference between the reference state and bake hardening annealed state. In other words, the BH-value describes the increase in the yield strength due to the bake hardening annealing.

$$\mathrm{BH}\ [\mathrm{MPa}] = R_{eL}\ (\text{with BH})\ [\mathrm{MPa}] - R_{P0.2}\ (\text{after prestrain})\ [\mathrm{MPa}] \quad (1)$$

$$\mathrm{BH}\ [\mathrm{MPa}] = R_{P0.2}\ (\text{with BH})\ [\mathrm{MPa}] - R_{P0.2}\ (\text{after prestrain})\ [\mathrm{MPa}] \quad (2)$$

In the aforementioned method, the evaluation the bake hardening effect requests subtracting the strength of different samples. In addition to that method, a second evaluation method was used.[24,25] The reference state in the latter method was determined by the true stress of the specimen at the prestrain level. After the prestrain, the bake hardening annealing was carried out on the same sample. Subsequently, the tensile test was conducted to evaluate the contribution of bake hardening treatment to the increase in the strength. The BH*-values were calculated using true stress–true strain curves according to Equation 3 in the case of a discontinuous yielding, and Equation 4 in the case of a continuous yielding is occurring.

$$\mathrm{BH}^*\ [\mathrm{MPa}] = R_{eL}\ (\text{with BH})\ [\mathrm{MPa}] - \varphi_{true}\ [\mathrm{MPa}] \quad (3)$$

$$\mathrm{BH}^*\ [\mathrm{MPa}] = R_{P0.2}\ (\text{with BH})\ [\mathrm{MPa}] - \varphi_{true}\ [\mathrm{MPa}] \quad (4)$$

To study the effect of prestrain on the bake hardening effect on the high-Mn steel, prestrain of 0.02, 0.10, 0.20, and 0.30 in true strain were applied. The bake hardening annealing was conducted at 120, 170, and 220 °C for 5 min up to 30 min in air atmosphere. Sample temperature was monitored by a thermal couple. The bake hardening treatment was carried out referring to the standard DIN EN 10325 and modified by the investigated parameters.[23]

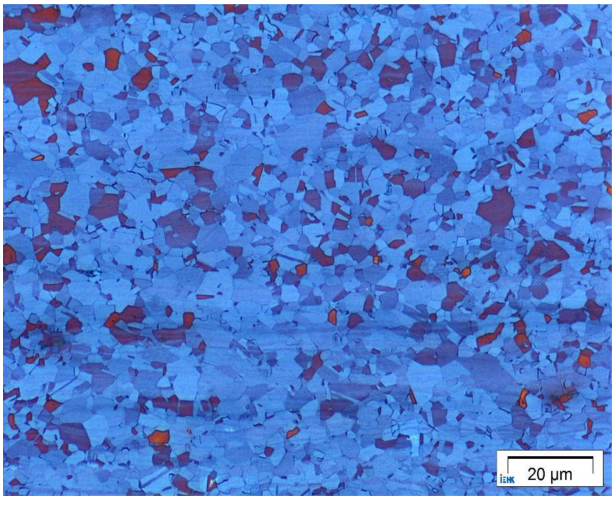

Figure 1. Microstructure conducted with Klemm etching of Fe–19 wt% Mn–0.4 wt%C–2 wt%Cr–1 wt%Al TWIP steel after skin-pass rolling.

2.2.2. Small Angle Neutron Scattering (SANS)

The SANS experiments were conducted at beamline KWS-2 of Jülich Centre for Neutron Science (JCNS) at Heinz Maier-Leibnitz Zentrum (MLZ), Garching, Germany. The wavelength of the neutron beam is $\lambda = 5$ Å. The samples were in dimensions of Ø8 mm × 1 mm and measured at two detection distances, namely 1.74 m for high Q-range and 7.74 m for low Q-range. The

collimation length is 8 m. The samples were measured in a 2.2 Tesla transversal magnetic field to the beam axis achieved with an electromagnet. Detailed information can be found somewhere else.[26]

3. Results

The BH-values and the BH*-values for the different combinations of prestrain, temperature and annealing time are given in **Table 1**. Considering the BH-value, there is nearly no increase in strength observed after a bake hardening treatment with 0.02 prestrain. The corresponding BH*-value is about 10 MPa. The increase in prestrain from 0.02 to 0.10 raises the BH-values within a range of 1–22 MPa. The increase in strength is more significant with higher annealing temperature. The highest BH-value achieves after an annealing at 200 °C with 0.10 prestrain. No strong influence of the annealing time is found. Compared with the BH-values, the regarding BH*-values are higher. The highest increase in strength is 56 MPa after an annealing at 200 °C with 0.10 prestrain. After 0.20 prestrain, BH-values increase and a maximum BH-value of 62 MPa is obtained at 200 °C annealing temperature. The difference between BH- and BH*-values is found to be ~10 MPa. A clear tendency of the increase in BH-values and BH*-values with the increasing annealing temperature is observed. The results of the tensile tests after bake hardening treatments with 0.30 prestrain differ from those with a smaller amount of prestrain. The BH-values show a different trend, compared with the BH*-values with the increase in the prestrain level. The BH-value is about 20 MPa after the bake hardening treatment with 0.30 prestrain. On the contrary, the BH*-value possesses a high value of about 110 MPa.

Table 1. BH-values and BH*-values calculated by Equation 1/2 and Equation 3/4, respectively, under various test conditions, the mean value of three parallel tests is provided.

Prestrain	Temperature [°C]	Annealing Time [min]	BH-value mean [MPa]	BH*-value mean [MPa]
0.02	170	10	1	12
		20	0	14
		30	1	10
0.1	120	10	1	35
		20	3	37
		30	2	39
	170	10	10	45
		20	12	46
		30	9	39
	200	10	22	56
		20	14	43
		30	19	43
0.2	120	10	32	42
		20	36	44
		30	35	46
	170	5	47	57
		10	51	60
		15	51	59
		20	49	55
		25	56	64
		30	55	65
		40	51	64
	200	10	56	66
		20	57	67
		30	62	66
0.3	170	10	16	103
		20	26	107
		25	24	110
		30	18	106
		40	8	101

3.1. The Influence of Prestrain on the Mechanical Properties

In order to study the influence of prestrain on the mechanical properties on the high-Mn TWIP steel, prestrain of 0.02, 0.10, 0.20, and 0.30 is applied to the specimens prior to bake hardening annealing. **Figure 2** displays the stress-strain curves after annealing at 170 °C for 20 min, in combination with the reference states (only prestrained without BH). The stress–strain curves after 0.02 prestrain before and after bake hardening annealing show no significant difference with a continuous yielding behavior. The combination of 0.10 prestrain with an annealing at 170 °C increases the yield strength by 12 MPa and affects the shape of the stress–strain curve. For the bake hardening annealed sample, the stress–strain curve displays a discontinuous yielding behavior with localized deformation. In addition, the bake hardening annealing results in an increase in total elongation from 34 to 36%. The most prominent change of the curve's shape is found after the bake hardening treatment with 0.20 prestrain. A discontinuous yielding is followed by a small drop in stress. After this local minimum in stress, a

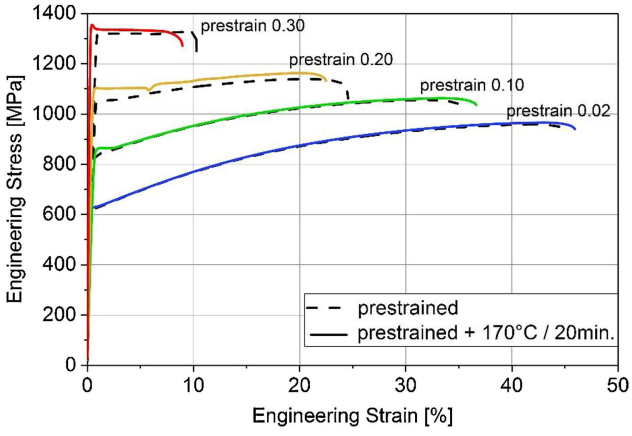

Figure 2. Stress–strain curves of the prestrained samples after an annealing at 170 °C for 20 min (dashed lines without annealing and colored solid lines with an annealing).

homogeneous flow is apparent. For specimens with 0.30 prestrain, the stress–strain curves show a minor difference in yield strength. The annealed as well as the unannealed states show a discontinuous yielding behavior. The annealed state develops a local maximum at onset of plastic flow and both prestrained and annealed states depict a limited strain hardening.

A detailed analysis on the yielding behavior is shown in **Figure 3**. It illustrates the response of the material to tensile deformation at the beginning of deformation. The three states shown here are: initial, prestrained + stored at room temperature (24 h) and prestrained + annealing at 170 °C for 20 min. The numbers describe the stress states used to calculate the BH-values and BH*-values as follows: 1) indicates the true stress of the material at a prestrain level; 2) describes the 0.2% proof stress of a prestrained sample; and 3) is the corresponding 0.2% proof strength/lower yield strength of the prestrained and bake hardening annealed sample. The BH-values were calculated by subtracting stress state 2 from state 3 and the BH*-values were calculated by subtracting the stress state 1 from state 3. Figure 3 further illustrates the change in the yielding behavior by the increase in prestrain. On the left side, the stress–strain curves of specimens with 0.02 prestrain are presented. The low prestrain (0.02) results in a continuous transition from elastic to plastic deformation. The stress–strain curves of state 2 and state 3 are nearly identical. On the right side of the figure, the curves of samples with 0.20 prestrain show a homogenous deformation. When the prestrained specimens are stored at room temperature for several hours afterwards, the yielding of the material is discontinuous but not pronounced. When an additional annealing is carried out at 170 °C for 20 min, a pronounced yielding is observed. In the diagram, there is plateau without the increase in strength for about 5% yield elongation, which is subsequently followed by a small drop in stress.

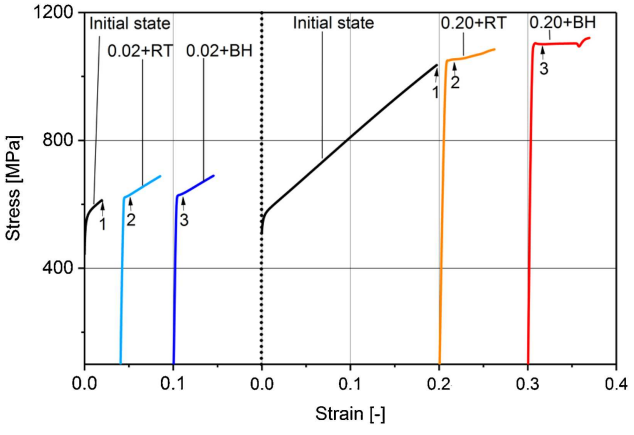

Figure 3. Difference in yield behavior before and after bake hardening annealing after prestrain of 0.02 and 0.20. (RT, room temperature).

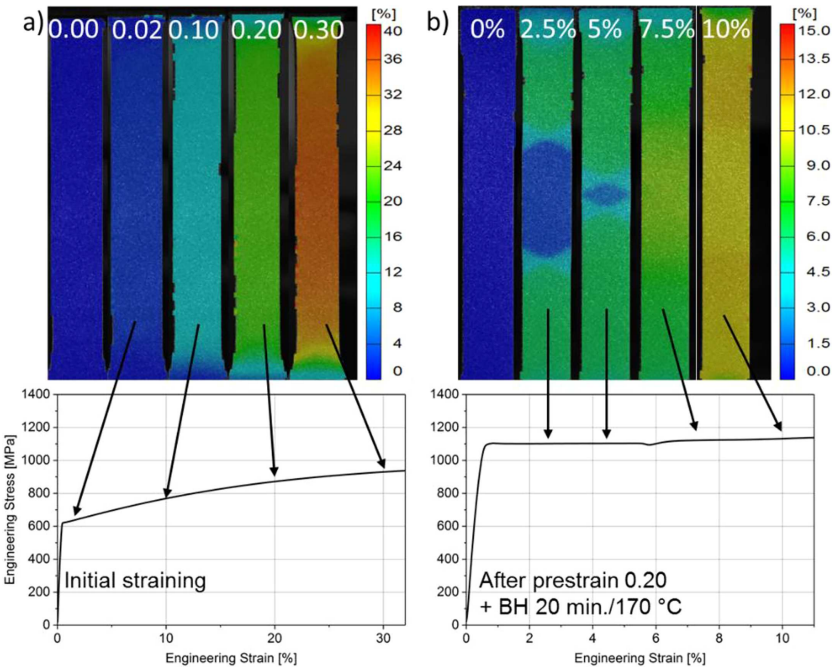

Figure 4. DIC analysis of the local strain distribution of tensile test specimens in a) the initial state and b) the prestrained state.

Figure 4 illustrates the local deformation behaviors of the high-Mn steel during prestrain and after the annealing using DIC analysis. As shown in Figure 4a, the sample in the initial state deforms homogeneously during prestraining. Even at a deformation degree of 0.30, neither localized deformation nor an inhomogeneous flow is observed. As mentioned above, the pronounced yielding phenomenon is observed when the sample is annealed at 170 °C for 20 min after 0.20 prestrain, which is reflected by strain localization. In this case, an inhomogeneous strain distribution on the specimen is observed, as shown in Figure 4b. Two deformation bands nucleate within the heads of the specimen and move toward the center of the gauge. The front of deformation bands shows an x shape. After 5% of the global strain, the bands converge in the middle of the specimen. Afterwards, the deformation bands disappear and the material deforms homogeneously. There are no further bands detected until specimen fracture.

3.2. Influence of Annealing Conditions

Besides the prestrain level, the annealing temperature has great influence on the mechanical properties as well. The BH-values as a function of the annealing temperature and the prestrain is shown in **Figure 5**. The dashed line represents the BH*-values after annealing at 170 °C. Further, the BH-values increase with higher annealing temperature. After 0.10 prestrain, as show in Figure 5, the BH-values increase from 3 to 14 MPa with the increase in temperature from 120 to 200 °C. The BH-values after 0.20 prestrain shows a similar trend as a function of annealing

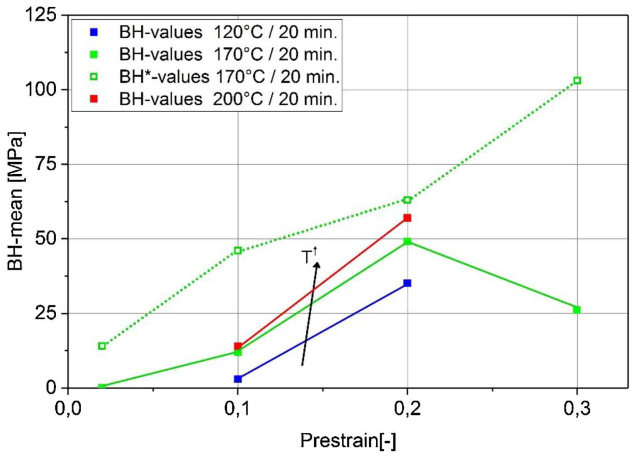

Figure 5. BH-values as a function of prestrain and annealing temperature after annealing for 20 min.

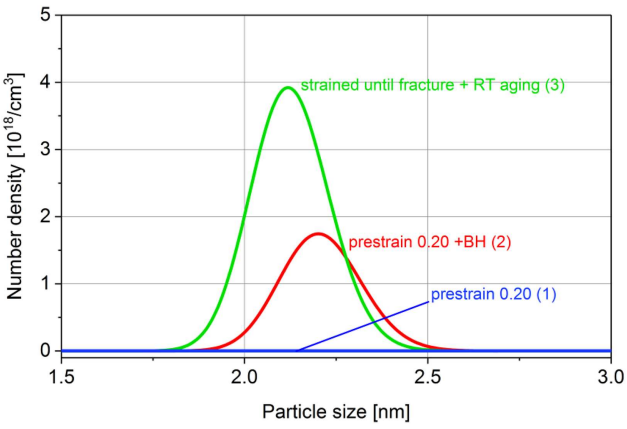

Figure 7. Development of number density and particle size at different combinations of prestrain and aging conditions. The numbers refer to explanations in the text. (RT, room temperature).

temperature. The increase in strength is calculated to be 36, 49, and 57 MPa after annealing for 20 min at 120, 170, and 200 °C, respectively. The influence of temperature is more distinctive at a higher prestrain level.

Figure 6a shows the BH-values as a function of annealing time. It can be seen that there is no significant change of the BH-values with the increase in annealing time. The results indicate that the annealing time does not play an important role in bake hardening effect of the investigated high-Mn steel. Figure 6b compares the formability of the annealed samples for different combinations of prestrain and annealing time at a temperature of 170 °C. The 0.10 prestrained and annealed samples still maintain about 35% elongation. After 0.20 prestrain, approximately 22% of formability can be achieved. No change in formability with the increase in annealing time is found for both cases. After 0.30 prestrain, the formability of the material declines strongly with the increase in annealing time. With increasing annealing duration from 10 to 30 min, the formability drops from 9.1 to 2.2%. After annealing at 170 °C for 40 min, the material has barely formability left and fails directly after the elastic deformation regime.

3.3. Results from Small Angle Neutron Scattering (SANS)

The results of the SANS measurements using specimens with different bake hardening treatments are depicted in **Figure 7**. After applying 0.20 prestrain (line 1), there is no scattering peak observed which indicates a negligible formation of Mn–C SRO in the materials at this state. Since room temperature aging might occur after prestrain, the prestrained specimen was cooled to −15 °C until the SANS measurement, in order to prevent the material from room temperature aging. As aging was suppressed, the number density of the Mn–C SRO is extremely small after 0.20 prestrain. When a subsequent annealing is applied at 170 °C for 20 min on the 0.20 prestrained specimen (2), the number density of the Mn–C SRO significantly increases to a value of $1.75^{*}10^{18}$ cm^{-3}. In order to investigate the influence of room temperature aging on the SRO formation, a bake-hardened specimen was elongated up to fracture and aged at room temperature for 5 days. Then the SANS measurement was performed on that sample. The corresponding scattering curve is illustrated by line (3). A number density of $3.92^{*}10^{18}$ cm^{-3} and a mean particle size of 2.12 nm is found. To conclude, small angle

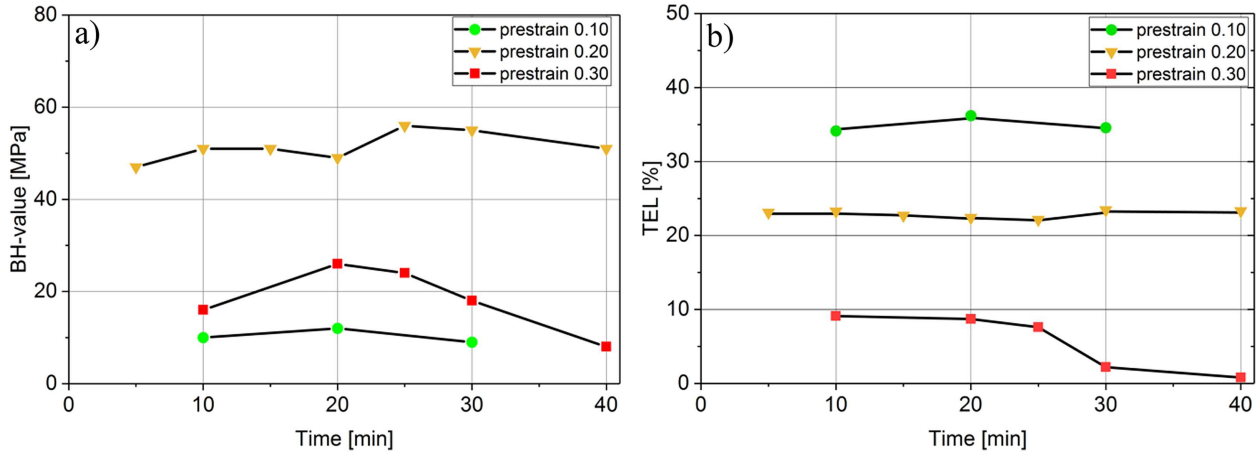

Figure 6. Development of a) the BH-values and b) the residual formability with increasing annealing time at 170 °C after prestrain 0.10, 0.20, and 0.30.

neutron scattering (SANS) measurements indicate the absence of short range ordering (SRO) after 0.20 prestrain; however, SRO re-occurs after the annealing. At high prestrain, an increase in the number density of Mn–C SRO is found in both cases – after annealing at elevated temperature and aging at room temperature, indicating an accelerated SRO.

4. Discussion

Comparing with the observations in austenitic Cr–Ni steels,[27,28] the pronounced yielding phenomenon in the high-Mn TWIP steel shows distinct characteristics. In austenitic Cr–Ni steels, the transformation induced plasticity (TRIP) effect takes place during prestrain and the strain-induced martensite might have great impact on the bake hardening effect. Because the α'-martensite with body-centered tetragonal structure provides a fast carbon diffusion condition. The bake hardening mechanism of the investigated purely austenitic high-Mn TWIP steel are different from that in Cr–Ni austenitic steels. In high-Mn TWIP steel Fe–19 wt%Mn–0.4 wt%C–2 wt%Cr–1 wt%Al, a certain combination of prestrain and annealing temperature is needed to increase the strength during a bake hardening treatment. After 0.10 prestrain, an annealing temperature of 120 °C is not sufficient to increase the strength. In comparison, after annealing at 170 °C strength is significantly increased, as most probably a certain combination of prestrain and temperature is needed. The 0.20 prestrained and annealed samples exhibit a pronounced yielding phenomenon, with x-shaped bands moving through the sample. The occurrence of bands during tensile tests was also observed in the same material in tensile tests at 170 °C (in a typical dynamic strain aging temperature range), which may have the same origin. The shape of the stress–strain curve after 0.30 prestrain without annealing also depicts a pronounced yielding (Figure 2). The pronounced yielding is a result of room temperature aging. The room temperature aging further leads to the deviating BH-values, as the 0.30 reference state unintentionally aged and thus the calculated reference yield stress is too high.

As shown in Figure 7, the bake hardening annealing results in the formation of Mn–C SRO. This formation comes along with an increase in yield strength of the 0.20 prestrained and bake hardening annealed sample, which is observed in the corresponding stress strain curves. In previous study, it was reported that C and Mn form stable clusters within the f.c.c. matrix.[19] It was found that these Mn–C SRO act as effective obstacles to the dislocation glide, an additional stress is needed to destroy the formed clusters.[18] Our study confirms that formed Mn–C SRO can be connected to an increase in the yield strength experimentally. As the 0.30 prestrained sample shows discontinuous yielding behavior even without bake hardening annealing, the room temperature aging might be the reason for that. To avoid room temperature aging, the prestrained sample was cooled down until SANS measurement and there were no Mn–C SRO observed in this specimen. On the contrary, there were a large number of Mn–C SRO found in the sample stored at room temperature for 5 days. The results indicate that the room temperature aging indeed takes place after prestrain. The formation of Mn–C SRO at room temperature might be due to the high dislocation density in the highly deformed sample. The room temperature aging has an impact on the reference state, which needs to be taken into account for the evaluation of the BH effect in high-Mn steel.

5. Conclusions

The TWIP steel Fe–19 wt%Mn–0.4 wt%C–2 wt%Cr–1 wt%Al was investigated by means of the uniaxial tensile tests with digital image correlation (DIC) in situ monitoring and small angle neutron scattering (SANS). For investigating the effects of bake hardening on the yield strength and ductility, various prestrain and bake hardening conditions were studied. The main conclusions are drawn as below:

1) With increasing prestrain, the BH-value of the investigated high-Mn TWIP steel increases. Large prestrains, that is, above approximately 0.30, even leads to room temperature aging.
2) The annealing temperature has significant influence on the yield strength. The higher annealing temperature results in a larger increase in the yield strength. The annealing time shows little influence on the BH-value and the yield strength.
3) Small angle neutron scattering (SANS) indicates that BH annealing results in the formation of a short range ordered Mn–C cluster. These nano-sized Mn–C SRO clusters form during the bake hardening treatment after 0.20 prestrain and contribute to the increase in yield strength.
4) The formation of Mn–C SRO is further detected after aging at room temperature. This room temperature aging leads to an increase in the yield strength of largely prestrained samples. In order to fully exploit the bake hardening effect, the room temperature aging needs to be avoided.

Acknowledgements

The authors gratefully acknowledge the financial support of the Deutsche Forschungsgemeinschaft (DFG) within the Collaborative Research Center (SFB) 761 "Steel – ab initio: quantum mechanics guided design of new Fe based materials." The SANS experiment support from the KWS-2 beamline of Jülich Centre for Neutron Science (JCNS) at Heinz Maier-Leibnitz Zentrum (MLZ) is gratefully acknowledged. The authors are also grateful for the support and helpful comments to C. Blankart, I. Gospodinov and T. Ingendahl of the Steel Institute of RWTH Aachen University.

Conflict of Interest

The authors declare no conflict of interest.

Keywords

Bake-hardening, High-Mn steel, Small angle neutron scattering (SANS), Static strain aging, TWIP steel

Received: November 28, 2017
Revised: January 17, 2018
Published online:

[1] W. Bleck, X. Guo, Y. Ma, *Steel Res. Int.* **2017**, *88*, 1.
[2] C. Haase, T. Ingendahl, O. Güvenç, M. Bambach, W. Bleck, D. A. Molodov, L. A. Barrales-Mora, *Mater. Sci. Eng. A* **2016**, *649*, 74.
[3] O. Grässel, L. Krüger, G. Frommeyer, L. W. Meyer, *Int. J. Plastic.* **2000**, *16*, 1391.
[4] H. Kim, D.-W. Suh, N. J. Kim, *Sci. Technol. Adv. Mater.* **2013**, *14*, 14205.
[5] V. Shterner, I. B. Timokhina, H. Beladi, *Mater. Sci. Eng. A* **2016**, *669*, 437.
[6] G. Frommeyer, U. Brüx, P. Neumann, *ISIJ Int.* **2003**, *43*, 438.
[7] H. Gwon, J.-K. Kim, B. Jian, H. Mohrbacher, T. Song, S.-K. Kim, B. C. de Cooman, *Mater. Sci. Eng. A* **2018**, *711*, 130.
[8] E. Pereloma, I. Timokhina, *Automotive Steels: Design, Metallurgy, Processing and Applications* (Eds: R. Rana, S.B. Singh), Woodhead Publishing, Duxford **2017**, pp. 259–288.
[9] S. Brühl, *Einfluss der Martensitphase auf das Bake-Hardening-Verhalten von Dualphasen-Stählen. Dissertation*, Shaker, Aachen **2011**.
[10] A. H. Cottrell, *London Edinburgh Dublin Philos. Mag. J Sci.* **1953**, *44*, 829.
[11] A. Ramazani, S. Bruehl, M. Abbasi, W. Bleck, U. Prahl, *Steel Res. Int.* **2016**, *87*, 1559.
[12] D. E. Jiang, E. A. Carter, *Phys. Rev. B* **2003**, *67*, 214103.
[13] T. Hickel, S. Sandlöbes, R. K. W. Marceau, A. Dick, I. Bleskov, J. Neugebauer, D. Raabe, *Acta Mater.* **2014**, *75*, 147.
[14] B. K. Zuidema, D. K. Subramanyam, W. C. Leslie, *MTA* **1987**, *18*, 1629.
[15] C. Wells, W. Batz, R. F. Mehl, *J. Met.* **1950**, *1950*, 553.
[16] R. Ruoppa, T. Taulavuori, *Presented at Conf. 6th European Stainless Steel Conference*, Helsinki **2008**.
[17] J. B. Seol, J. G. Kim, S. H. Na, C. G. Park, H. S. Kim, *Acta Mater.* **2017**, *131*, 187.
[18] J.-H. Kang, T. Ingendahl, J. von Appen, R. Dronskowski, W. Bleck, *Mater. Sci. Eng. A* **2014**, *614*, 122.
[19] J. von Appen, R. Dronskowski, *Steel Res. Int.* **2011**, *82*, 101.
[20] T. A. Timmerscheidt, R. Dronskowski, *Steel Res. Int.* **2017**, *88*, 1.
[21] S. Kilic, F. Ozturk, T. Sigirmac, G. Tekin, *J. Iron Steel Res. Int.* **2015**, *22*, 361.
[22] A. Saeed-Akbari, L. Mosecker, A. Schwedt, W. Bleck, *Metall. Mat. Trans. A* **2012**, *43*, 1688.
[23] DIN Deutsches Institut für Normung e. V., DIN German Institute for Standardization, *Determination of Yield Strenght Increase by the Effect of Heat Treatment (Bake-Hardening-Index) Deutsche Fassung EN 10325:2006*, Beuth Verlag GmbH, Berlin, *77.040.10; 77.080.20* **2006**.
[24] I. B. Timokhina, P. D. Hodgson, E. V. Pereloma, *Metall. Mat. Trans. A* **2007**, *38*, 2442.
[25] W. Bleck, S. Brühl, T. Gerber, *Control and Exploitation of the Bake-Hardening Effect in Multi-Phase High-Strength Steels: Final Report*, EUR-OP, Luxembourg **2007**.
[26] W. Song, A. Radulescu, L. Liu, W. Bleck, *Steel Res. Int.* **2017**, *88*, 1700079.
[27] T. Juuti, L. P. Karjalainen, R. Ruoppa, T. Taulavuori, *MSF* **2010**, *638-642*, 3278.
[28] P. Antoine, B. Soenen, N. Akdut, *MSF* **2007**, *539-543*, 4891.

